Contact Resistance in RFID Chip-Antenna Interfaces

by

Chetak M. Reshamwala

SUBMITTED TO THE DEPARTMENT OF MECHANICAL ENGINEERING
IN PARTIAL FULFILLMENT OF THE REQUIREMENTS FOR THE DEGREE OF

BACHELOR OF SCIENCE IN MECHANICAL ENGINEERING
AT THE
MASSACHUSETTS INSTITUTE OF TECHNOLOGY

JUNE 2001

Signature of Author: _____
Department of Mechanical Engineering
May 11, 2001

Certified by: _____
Sanjay Sarma
Professor of Mechanical Engineering
Thesis Supervisor

Accepted by: _____
Ernest G. Cravalho
Professor of Mechanical Engineering
Chairman, Undergraduate Thesis Committee

Contact Resistance in RFID Chip-Antenna Interfaces

by

Chetak M. Reshamwala

Submitted to the Department of Mechanical Engineering
on May 11, 2001, in partial fulfillment of the
requirements for the Degree of Bachelor of Science in
Mechanical Engineering

ABSTRACT

The purpose of this study was to determine a force-deflection relationship and a force-contact area relationship between a flat planar solid and a spherical solid in terms of material and surface properties of the two bodies. This relationship was determined and it was discovered that the force was directly proportional to both the deflection and contact area. This information is useful in the design and performance of RFID chips. The RFID chip-antenna interface is the area of greatest power loss in the system, and by determining a relationship to increase the contact area in that region, the power loss to the antenna can be reduced.

Moreover, an analysis including asperities on the micro scale geometry of the solids was conducted. In the final approach to the problem, a random distribution of asperity types was analyzed. An expression was derived for the total force applied in terms of a given deflection and a range of asperity radii of curvature. A three-dimensional graph was created to show how each of these variables depends on the each other when asperities exist. This relationship is very significant, because it can be used to improve current RFID chip technology to achieve better performance. This expression can also be used to determine specifications in the manufacturing process to achieve a certain deflection or area of contact between the contacting bodies, thereby improving the current manufacturing process.

Thesis Supervisor: Sanjay Sarma
Title: Professor of Mechanical Engineering

Table of Contents

Figures and Tables

1.0 Introduction

It is the goal of the Auto-ID Center at MIT to reduce the power loss through an RFID chip-antenna interface due to the adhesive bond between the two surfaces. There is a direct correlation between how much power the antenna receives and how well it recognizes a signal. Therefore, it is desired to get as much power to the antenna as possible. Unfortunately, adhesive bonds are inherently non-conductive, and therefore the area of greatest resistance is between the RFID chip and the antenna. If the contact resistance can somehow be lowered, then the power loss can be lowered also.

One way in which the contact resistance can be lowered is to increase the contact area between the two surfaces, thereby allowing more current flow per unit area. The contact resistance is indirectly proportional to the contact area between the surfaces in contact. For example, the greater the contact area is between the chip and the antenna, the lower the electrical resistance is between the two contacting bodies. The smaller is the contact area, the higher is the electrical resistance. Since the goal is to decrease the power loss, it is desired to decrease the resistance, and therefore increase the contact area.

In order to do so, one must first understand the relationship between the force applied between the two solids, the deflection of the two solids, and the contact area that arises as a result of the force applied between the two solids. This study will attempt to determine idealized relationships relating these three parameters.

Finally, when dealing with micro scale geometry, asperities on the surface become an issue in determining the force applied, deflection, and size of the contact area between the two solids. This study will further investigate the effects of asperities on the relationships between the force, deflection, and contact area of contacting bodies.

2.0 Statement of Problem

There are two small spherical objects on the top of the RFID chip that come into contact with the flat antenna. The antenna exerts a force on the spherical objects on the chip, and contact stresses arise between the RFID chip-antenna interfaces. Figure 1 shows a sketch of the RFID chip-antenna assembly, and shows the location of the contact stresses of interest in this study.

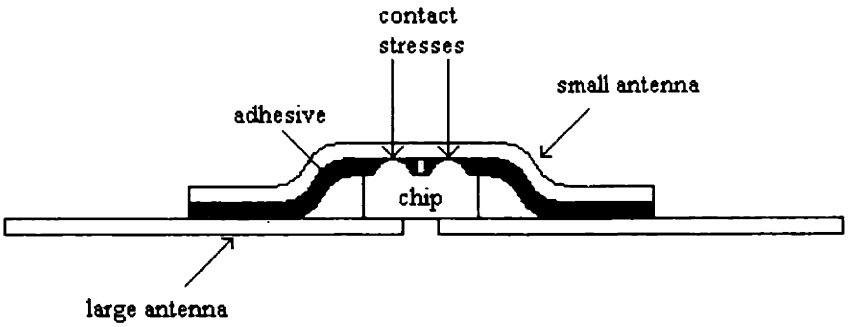

Figure 1: Sketch of RFID chip-antenna assembly and location of contact stresses (not drawn to scale).

It is possible to decrease the resistance through the chip-antenna interface by increasing the contact area in the interface without plastic deformation of the solids. The objective of this study is to determine relationships describing this phenomenon.

The geometry consists of a flat planar solid coming into contact with a spherically shaped solid. It is desirable to determine the relationship between the force applied on the chip-antenna interface, the total deflection of the two solids that occurs as a result of this force, and the size of the contact area between the two solids. This relationship can be determined using Hertz theory of elastic contact between two smooth solids.

In addition, asperities are introduced to the small-scale geometry of the spherical solid to determine the effect of small deviations of the surface profile on the force, deflection, and contact area between the two solids. An analysis is conducted to determine the relationship between the size of an asperity, and its force-deflection relationship.

Finally, it is assumed that there is a random distribution of asperity types. Therefore, an expression is needed to determine the total force applied given in terms of the total deflection and a range of asperity types on the surface of the spherical solid.

3.0 Theoretical Analysis

3.1 Geometry of Smooth Surfaces in Contact

When two solids are brought into contact, they initially touch at a single point or along a line. In the case of the RFID chip-antenna interface, a flat planar body comes into contact with a spherical body. In this case, the initial contact area is a single point. Under the smallest load, both bodies begin to deform in the vicinity of the first point of contact, so that the two bodies now touch over a finite area. A theory of normal contact of elastic solids (Hertz theory) is used to determine the size and shape of the contact area and how it grows with increasing load. Figure 2 shows two bodies coming into contact, a plane and a sphere, and how the shape of the sphere changes with increasing load from the planar body, as well as how the contact area grows with increasing load.

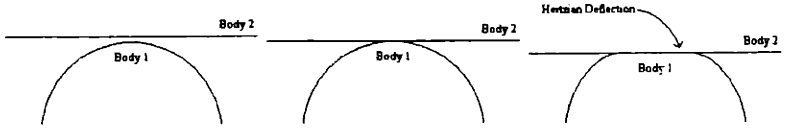

Figure 2: A planar body coming into contact with a spherical body.

Figure 3 below shows two solids of general shape in cross-section after deformation (adapted from [2]). The first point of contact is the origin of a rectangular coordinate system, where the x-y plane is the common tangent plane to the two surfaces and the z-axis lies along the common normal to the two surfaces. The z-axis is positive into the lower solid. Each surface is smooth on both the micro and macro scale. On the micro scale, this means the absence of small surface asperities that may lead to discontinuous contacts or local variations in contact pressure.

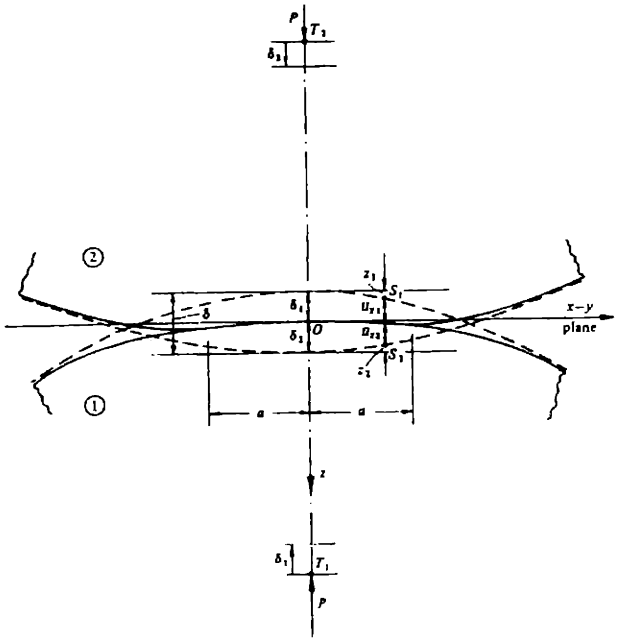

Figure 3: Two solids of general shape in cross-section after deformation (adapted from [2]).

Hertz theory was used here to determine a relationship between the total force, F, between the two bodies, the total deflection, δ, of the two bodies, and the radius of the contact area, a, between the two bodies. Some assumptions that were made to idealize the properties of the contacting bodies and the contact conditions are ([1]):

- the contacting bodies are elastic, homogeneous, and isotropic,
- the strains are small,
- the surfaces are smooth and non-conforming,
- the surface shape does not change in time, and
- the contact is frictionless.

The profile of each surface in the region around the origin can approximately be expressed by an expression of the form,

$$z_1 = A_1 x^2 + B_1 y^2 + C_1 xy + \ldots, \tag{3.1}$$

where higher order terms in x and y are neglected. Choosing the orientation of the x and y axes, so that the term in xy vanishes, (3.1) can be written,

$$z_1 = \frac{1}{2R_1'} x^2 + \frac{1}{2R_1''} y^2, \tag{3.2}$$

where R_1' and R_1'' are the principal radii of curvature of the surface at the origin. They are the maximum and minimum values of the radius of curvature of all possible cross-sections of the profile. In the same way, an expression can be written for the second surface,

$$z_2 = -\left(\frac{1}{2R_2'} x^2 + \frac{1}{2R_2''} y^2 \right). \tag{3.3}$$

The separation between the two surfaces is the given by,

$$h = z_1 - z_2 = \frac{1}{2R_1'} x^2 + \frac{1}{2R_1''} y^2 + \frac{1}{2R_2'} x^2 + \frac{1}{2R_2''} y^2 = \frac{1}{2R'} x^2 + \frac{1}{2R''} y^2, \tag{3.4}$$

where R' and R'' are defined as the principal relative radii of curvature, given by,

$$\begin{aligned} \frac{1}{R'} &= \frac{1}{R_1'} + \frac{1}{R_2'} \\ \frac{1}{R''} &= \frac{1}{R_1''} + \frac{1}{R_2''} \end{aligned}. \tag{3.5}$$

Consider now the deformation as a normal load, F, is applied. Before deformation, the separation between two corresponding surface points $S_1(x, y, z_1)$ and $S_2(x, y, z_2)$ is given by (3.4).

From the symmetry of this expression about O, the contact region extends an equal distance on either side of O. During the compression, distant points in the two bodies T_1 and T_2 move towards O, parallel to the z-axis, by displacements δ_1 and δ_2 respectively. If the solids did not deform, their profiles would overlap as shown by the dotted lines in Figure 3. Due to the contact pressure applied, the surface of each body is displaced parallel to Oz by an amount u_{z1} and u_{z2} (measured positive into each body) relative to the distant points T_1 and T_2. If, after deformation, the points S_1 and S_2 are coincident within the contact surface, then,

$$u_{z1} + u_{z2} + h = \delta_1 + \delta_2 . \tag{3.6}$$

Writing $\delta = \delta_1 + \delta_2$ and using (3.4), an expression for the elastic displacement can be obtained,

$$u_{z1} + u_{z2} = \delta - \frac{1}{2R'}x^2 - \frac{1}{2R''}y^2 . \tag{3.7}$$

3.2 Elastic Deformation of Solids of Revolution

If the two bodies are solids of revolution, or spherical, then:

$$\begin{aligned} R_1' &= R_1'' = R_1 \\ R_2' &= R_2'' = R_2 \end{aligned} , \tag{3.8}$$

where R_1 and R_2 are the radii of curvature of body 1 and body 2 respectively. After loading, it is clear from the spherical geometry of the solids that the contact area will be circular, having a radius a. Therefore,

$$u_{z1} + u_{z2} = \delta - \frac{1}{2R}r^2 , \tag{3.9}$$

where,

$$\begin{aligned} \frac{1}{R} &= \frac{1}{R_1} + \frac{1}{R_2} . \\ r^2 &= x^2 + y^2 \end{aligned} \tag{3.10}$$

The pressure distribution proposed by Hertz ([2]) that gives rise to displacements that satisfy (3.9) is given by the following expression,

$$p = p_0 \left(1 - \left(\frac{r}{a} \right)^2 \right)^{1/2} , \tag{3.11}$$

where p_0 is the maximum pressure. This pressure distribution gives normal displacements,

$$u_z = \frac{1-\nu^2}{E}\frac{\pi p_0}{4a}\left(2a^2 - r^2\right). \tag{3.12}$$

Since the pressure acting on the second body is equal to the pressure acting on the first body,

$$\frac{1}{E^*} = \frac{1-\nu_1^{\,2}}{E_1} + \frac{1-\nu_2^{\,2}}{E_2}. \tag{3.13}$$

Substituting the expressions for u_{z1} and u_{z2} into (3.9),

$$\frac{\pi p_0}{4aE^*}(2a^2 - r^2) = \delta - \left(\frac{1}{2R}\right)r^2, \tag{3.14}$$

from which the radius of the contact circle is given by,

$$a = \frac{\pi p_0 R}{2E^*}, \tag{3.15}$$

and the approach of distant points in the two solids is given by,

$$\delta = \frac{\pi a p_0}{2E*}. \tag{3.16}$$

The total load compressing the solids is related to the pressure by,

$$F = \int_0^a p(r)2\pi r dr = \frac{2}{3}p_0 \pi a^2. \tag{3.17}$$

The maximum pressure p_0 is 3/2 times the mean pressure p_m. In most cases, the total load is usually specified, so that it is convenient to use (3.17) in combination with (3.15) and (3.16) to obtain,

$$a = \left(\frac{3FR}{4E^*}\right)^{1/3} \tag{3.18}$$

$$\delta = \frac{a^2}{R} = \left(\frac{9F^2}{16RE^{*2}}\right)^{1/3} \tag{3.19}$$

$$p_0 = \frac{3F}{2\pi a^2} = \left(\frac{6FE^{*2}}{\pi^3 R^2}\right)^{1/3} \tag{3.20}$$

These expressions provide values for the contact size, compression, and maximum pressure of solids of revolution in elastic contact.

Equations (3.18) and (3.19) can be rewritten solving for the force F to obtain,

$$F = \frac{4E^*}{3R}a^3 \tag{3.22}$$

$$F = \left(\frac{16RE^{*2}}{9}\delta^3\right)^{1/2} \tag{3.23}$$

Therefore, from (3.22) and (3.23), given E^* and the radii of curvature of both solids, the force needed to obtain a desired contact area (in terms of the radius of the contact area), or a desired deflection can be determined.

3.3 Introducing Asperities to the Micro Scale Geometry

In the analysis above, it was assumed that small surface asperities on the micro scale that may lead to discontinuous contacts or local variations in contact pressure did not exist. In this section, small surface asperities will be introduced to the micro scale geometry. The goal of this section is to determine new expressions relating force, deflection, and the radius of the contact area of two elastic solids in contact.

Asperities have various shapes and sizes. Their heights vary from a fraction of a nanometer to several millimeters. In the case of an RFID chip, the asperities of concern are on the order of 1 to 11 micrometers. Figure 4 shows a sketch of a spherical body now with asperities on it. It is clear from the sketch that the contact area will change given a non-smooth surface geometry.

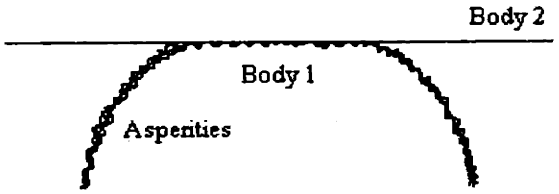

Figure 4: A planar body in contact with a spherical body with asperities.

3.3.1 First Case: Three Different Types of Asperities

In this first case, the effects of three different types of asperities on the surface of the spherical body will be examined. It will be assumed that each asperity is a cylinder of diameter and height h, with a half-spherical top of radius of curvature r. The radius of curvature is therefore given by,

$$r = \frac{h}{2}. \tag{3.24}$$

Therefore, the taller is the asperity, the larger is its radius of curvature. In the same way, the shorter is the asperity, the smaller is its radius of curvature. This relationship is shown in Figure 5 below.

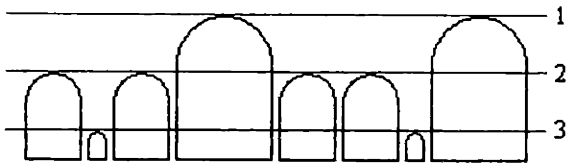

Figure 5: Asperity height/radius of curvature relationship.

In order to determine the force on each of the tallest asperities as a function of deflection, we use (3.23). The expression is

$$f_1 = \left(\frac{16 r_1 E^{*2}}{9} \delta^3 \right)^{1/2}. \tag{3.25}$$

If there are N_1 tallest asperities, the total force applied is

$$F = N_1 f_1. \tag{3.26}$$

If the deflection due to the force applied is greater than the distance from line 1 to line 2 in Figure 5, then it is desirable to determine the force applied on each of the mid-sized asperities as a function of deflection. The distance from line 1 to line 2 is

$$\delta_{1,2} = \frac{3}{2}(h_1 - h_2). \tag{3.27}$$

Therefore, the expression relating force to deflection for the mid-sized asperities is

$$f_2 = \left(\frac{16 r_2 E^{*2}}{9} \left(\delta - \frac{3}{2}(h_1 - h_2) \right)^3 \right)^{1/2}. \tag{3.28}$$

With this slight modification of the force-deflection relationship for the mid-sized asperities, any value of the force f_2 in which there is an imaginary part implies that the flat surface has not yet reached the level of the mid-sized asperities. For N_2 mid-sized asperities, the total force applied is

$$F = N_1 f_1 + N_2 f_2. \tag{3.29}$$

Finally, the expression relating force to deflection for the short asperities is

$$f_3 = \left(\frac{16 r_3 E^{*2}}{9} \left(\delta - \frac{3}{2}(h_1 - h_3) \right)^3 \right)^{1/2}, \tag{3.30}$$

where the total force applied is

$$F = N_1 f_1 + N_2 f_2 + N_3 f_3 . \tag{3.31}$$

Since the force f is a function of both the deflection δ and the asperity radius of curvature r, a three-dimensional graph can be created to see the relationship between these three parameters on a per asperity basis. This graph is discussed in the Results section. The next section describes how to deal with a random distribution of asperity types.

3.3.2 Second Case: Random Distribution of Asperity Types

For the case of a random distribution of asperity types (i.e., random radii of curvature and corresponding heights), it is assumed that the surface profile $y(x)$ is a random process that possesses a probability density function $\phi(y)$, where $\phi(Y)$, for example, is the probability that $y \leq Y$.

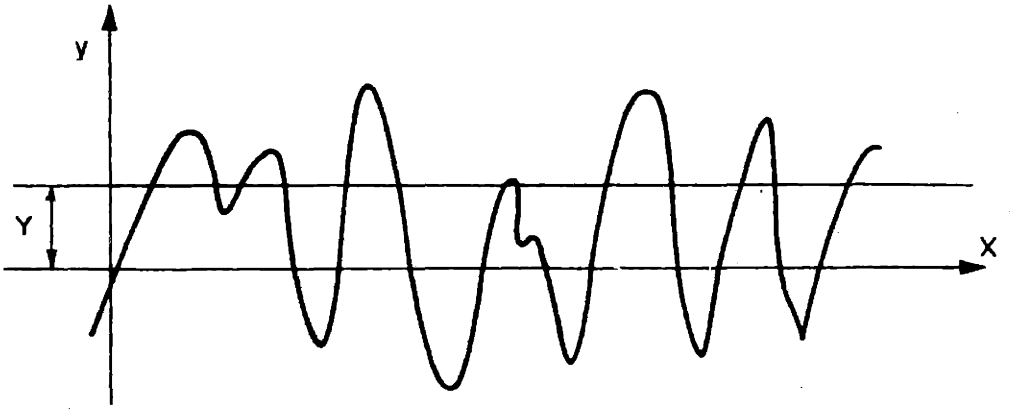

Figure 6: Random process of surface profile.

It will be assumed that the surface height is normally distributed, and hence the asperity radii of curvature on the surface are also normally distributed. Figure 7 on the next page gives an example of a graph of the random distribution of asperity types on the surface of a spherical solid body. Most of the asperities are within the range of 3 μm to 9 μm, and there are fewer asperities below 3 μm and above 9 μm.

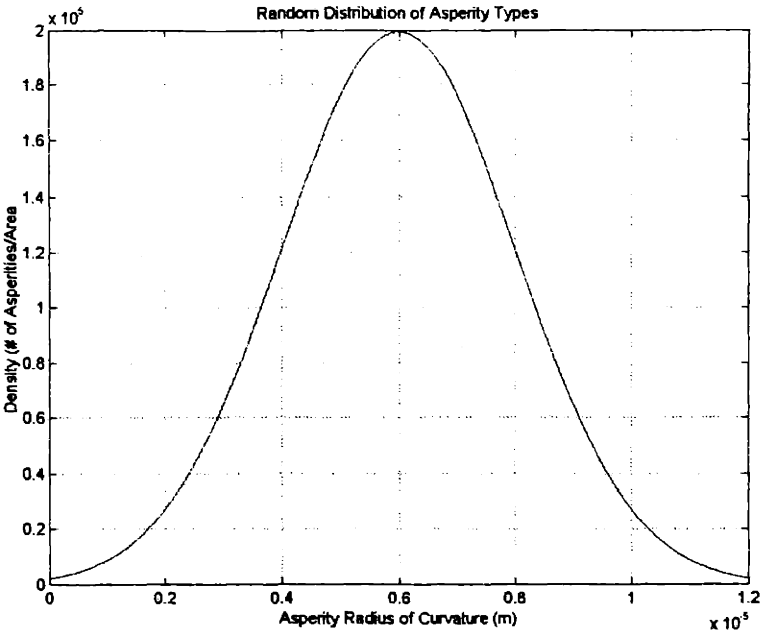

Figure 7: Random distribution of asperity types.

The distribution has a mean, μ, of 6 μm, and a standard deviation, σ, of 2 μm. The probability density function of the number of asperities per unit area is defined as,

$$N(r) = \frac{e^{\frac{-(r-\mu)^2}{2\sigma^2}}}{\sigma\sqrt{2\pi}}. \tag{3.32}$$

In the case of a random distribution of asperity heights, using (3.24) with (3.28), the force on one asperity is,

$$f(\delta, r) = \left(\frac{16 r E^{*2}}{9} (\delta - 3(r_{max} - r))^3 \right)^{1/2}, \tag{3.33}$$

where r_{max} is the radius of curvature of the largest asperity. Plugging in values for the parameters and variables, any value of f with an imaginary part should be ignored. The assumption is that if a value of f has an imaginary part, then the flat planar surface providing the load on the spherical body with asperities has not yet reached the top of the asperity of radius of curvature r used to determine f.

Using (3.32) and (3.33), an equation of the total force applied, F, in terms of a given deflection, σ, and a range of asperity radii of curvature, r, from μ-3σ to μ+3σ can be determined. Integrating over the range of values μ-3σ to μ+3σ,

$$F = \int_{\mu-3\sigma}^{\mu+3\sigma} \frac{e^{\frac{-(r-\mu)^2}{2\sigma^2}}}{\sigma\sqrt{2\pi}} \cdot \left(\frac{16rE^{*2}}{9} (\delta - (r_{max} - r))^3 \right)^{1/2} dr . \quad (3.34)$$

This equation ultimately defines the load needed to achieve a certain deflection given a range of asperities on the surface of an elastic solid in contact with another elastic solid. The equation can be manipulated in MATLAB or Maple to derive a numerical value for F given the system parameters.

4.0 Results

4.1 Elastic Deformation Analysis without Asperities

In the case of an RFID chip-antenna interface, the contact area needed to obtain a desired resistance will be given, and the force needed to create this contact area will be determined. Since we are dealing with a planar surface contacting a spherical surface, the radius of curvature of the planar surface, R_2, equals infinity, and $1/R_2$ therefore equals zero. As a result, from (3.10), $R = R_1$. In the following analysis, the radius of curvature of the spherical surface will be given on the order of $R = 0.05$ mm.

Moreover, in order to determine E^*, materials must be chosen for body 1 and body 2. Aluminum will be used for the spherical body, and steel will be used for the planar body. Table 1 gives the values of Young's modulus and Poisson's ratio for aluminum and steel.

	E (GN/m^2)	ν
Aluminum: Pure and Alloy	68-78.6	0.32-0.34
Steel: Carbon and Low Alloy	193-220	0.26-0.29

Table 1: Material properties of aluminum and steel.

Given these values, $E^* = 57.4$ GN/m^2. Now that these values are known, using (3.22), a graph was created of the force desired versus the radius of the contact area for three different values of the radius of curvature of the spherical body. The graph is shown in Figure 8 below.

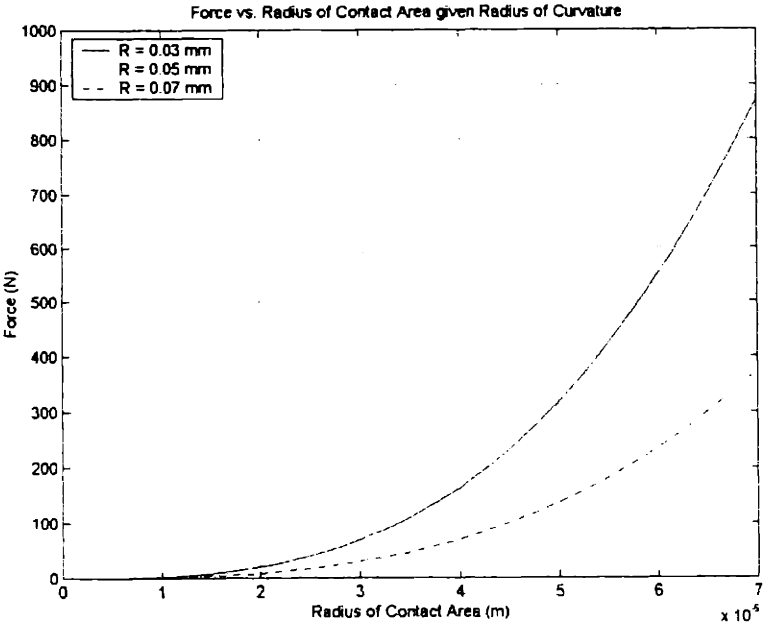

Figure 8: Force vs. radius of contact area given radius of curvature.

According to the graph, force increases as the radius of contact area increases, slowly at first, and more rapidly later. Also, as the radius of curvature increases, the curves become shallower.

Figure 9 is a similar graph. It plots force vs. deflection for three different radii of curvature. Once again, the force increases as the desired deflection increases. And as in the previous graph, the curves become shallower as the radius of curvature of the spherical body increases.

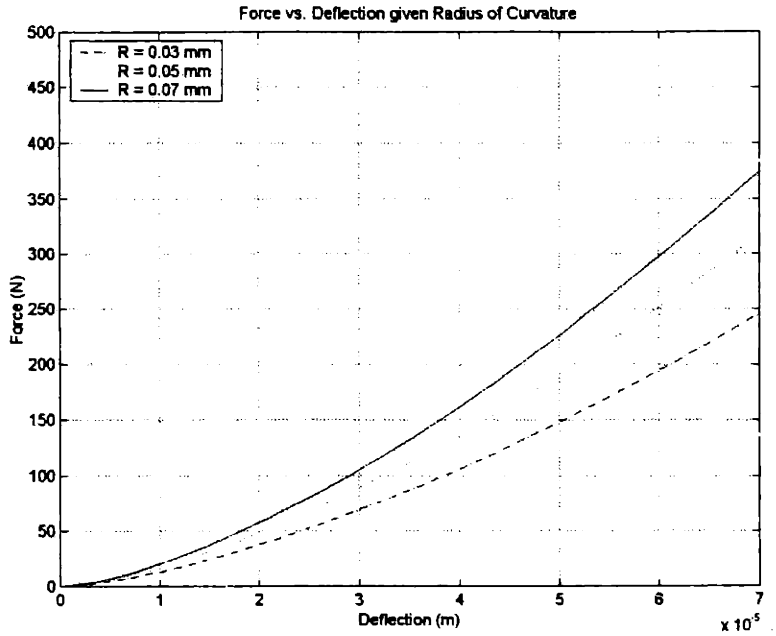

Figure 9: Force vs. deflection given radius of curvature.

4.2 Elastic Deformation Analysis with Asperities

In the following three graphs, the introduction of asperities into the situation is discussed. Figure 10 is a graph of the theoretical results from section 3.3.1. Figure 10 plots force vs. deflection on one asperity given its height and corresponding radius of curvature. The figure analyzes three different asperity types. One can deduce from the graph that the starting point of each curve depends on the size of the asperity. For example, the smaller is the asperity, the later is its starting point, because the planar surface contacts it later. And there is no force on the smaller asperities until the deflection increases to a certain point. After the starting point, each curve follows the basic force-deflection relationship, and the force increases with increasing deflection.

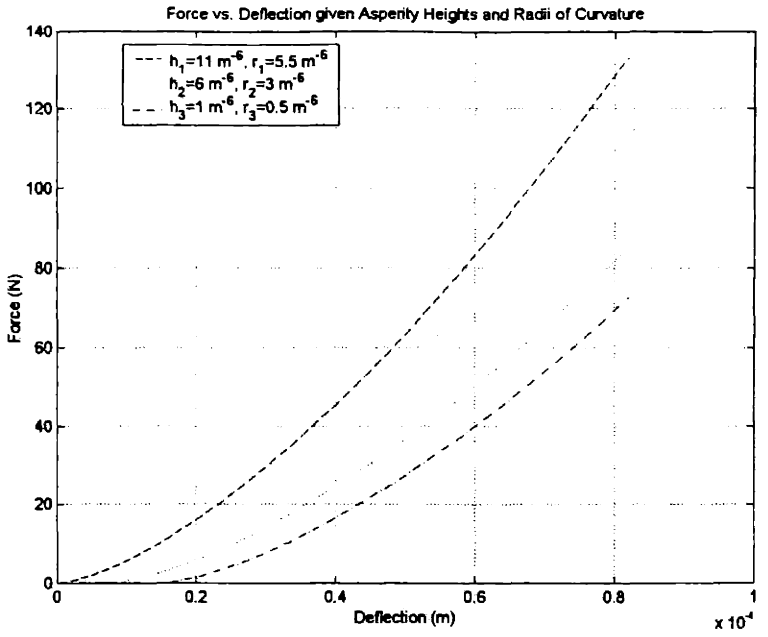

Figure 10: Force vs. deflection for one asperity given its height and corresponding radius of curvature.

Figure 11 plots the three curves in Figure 10, as well as a curve of the total force given one tall asperity, two mid-sized asperities, and one small asperity. The curve was determined using superposition. In a practical problem, however, there would be something on the order of 500 tall asperities, 1000 mid-sized asperities, and 500 small asperities. However, it was done this way in Figure 11 to show all four curves on a single plot. In the real case, the solid line representing the total force would be off the scale of the given axes.

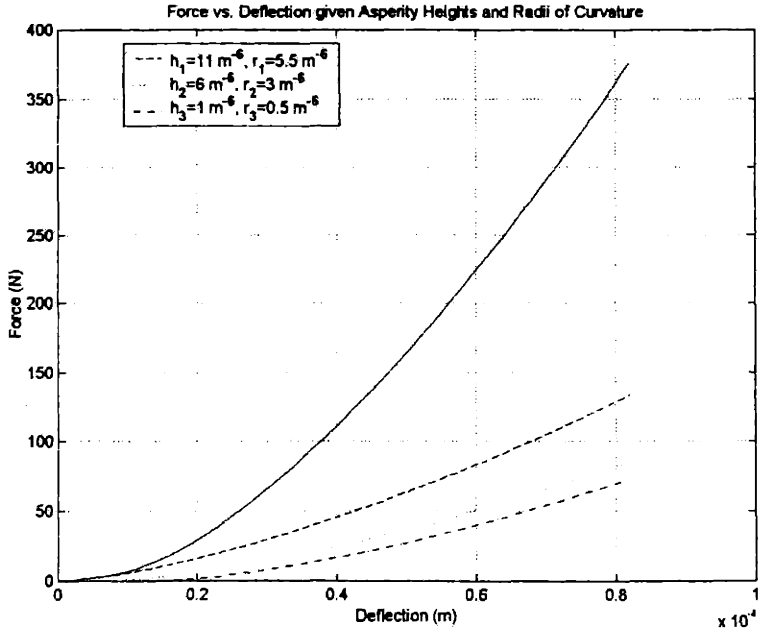

Figure 11: Total force vs. deflection given an asperity distribution (1,2,1).

Since the force, f, on one asperity is a function of both the deflection, δ, on that asperity as well as the radius of curvature, r, of the asperity, a three-dimensional graph can be created to observe the relationship between these three parameters on a per asperity basis. Figure 12 shows the three-dimensional graph; it summarizes the relationships of force, deflection, and asperity radius of curvature, on one graph.

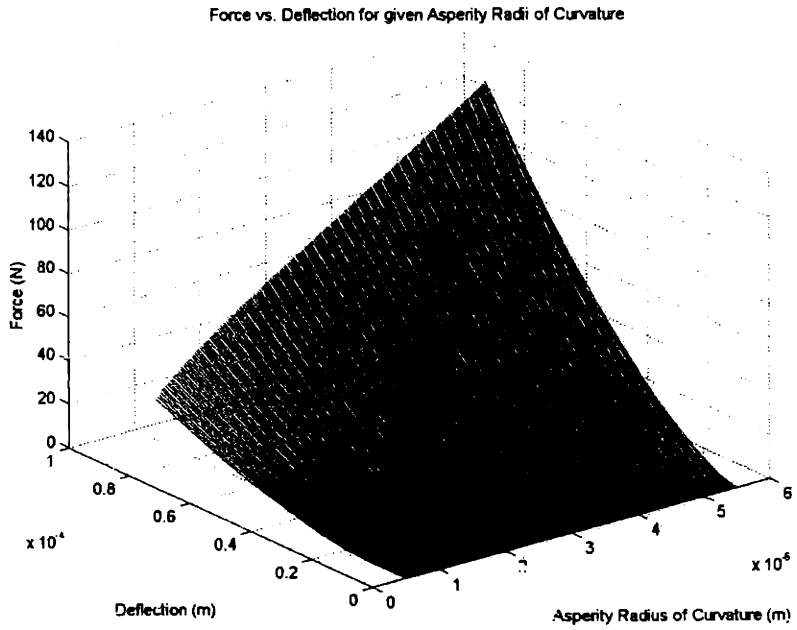

Figure 12: Force vs. deflection per asperity given asperity radius of curvature.

5.0 Conclusion

The purpose of this study was to determine a force-deflection relationship and a force-radius of contact area relationship between a flat planar solid and a spherical solid in terms of material and surface properties of the two solids. This relationship was determined and it was discovered that the force was directly proportional to both the deflection and contact area.

When asperities arose on the micro scale geometry, a modified force-deflection relationship was derived to determine the force applied on one asperity given the geometrical properties of the asperity and the deflection of the contacting bodies. A model of contacting bodies with asperities was created. Three different types of asperities on the surface of the spherical body were analyzed as a first-case approach to the problem to determine the effects of the asperities on the system variables. A new model of the shape of an asperity was created for ease of calculation. A graph was created to describe this relationship. In fact, it was determined that each asperity is independent of each other, and the total force applied is equal to the superposition of the individual forces on each asperity multiplied by the density (or number) of that specific type of asperity in a given area.

In the second-case approach to the problem, a random distribution of asperity types was used. An expression was derived for the total force applied in terms of a given deflection and a range of asperity radii of curvature. A three-dimensional graph was created to show how each of these variables depends on the other two when asperities exist.

This relationship is very significant, because it can be used to improve the current technology by changing certain geometrical or material properties of the solids to achieve better performance. This expression can also be used to determine the specifications in the manufacturing process to achieve a certain deflection or area of contact between the contacting bodies, thereby improving the current manufacturing process.

Finally, there are a few areas in which further research in this study would be beneficial. One area is in experimentally verifying the relationship between contacting bodies with asperities to determine how well the theoretical model compares to the experimental results. Another area of research could be in changing the geometrical properties or material properties of the contacting bodies, and then experimentally determining if there was a desired improvement or not in the chip performance. For example, by increasing the surface finish on the contacting bodies, one may be able to lose some of the asperities and increase the contact area between the surfaces. Still further research could be done in investigating conductive adhesives to attach the RFID chip to the antenna, thereby decreasing the resistance between the surfaces and improving the chip performance.

6.0 References

1. Goryacheva, I. G., *Contact Mechanics in Tribology*, Boston, Kluwer Academic Publishers, 1998.

2. Johnson, K. L., *Contact Mechanics*, New York, Cambridge University Press, 1985.

3. Mikic, Boriboje B. and Rohsenow, Warren M., *Thermal Contact Resistance*, Technical Report No. 4542-41, Department of Mechanical Engineering, MIT, 1966.